Single Chain Dynamic Structure Factor of Linear Polymers in an All-Polymer Nano-Composite

Arantxa Arbe,[*,†] José A. Pomposo,[†,‡,¶] Isabel Asenjo-Sanz,[†] Debsindhu Bhowmik,[§,‖] Oxana Ivanova,[⊥] Joachim Kohlbrecher,[#] and Juan Colmenero[†,‡,§]

Centro de Física de Materiales (CFM) (CSIC–UPV/EHU) – Materials Physics Center (MPC), Paseo Manuel de Lardizabal 5, 20018 San Sebastián, Spain, Departamento de Física de Materiales (UPV/EHU), Apartado 1072, 20080 San Sebastián, Spain, IKERBASQUE - Basque Foundation for Science, María Díaz de Haro 3, 48013 Bilbao, Spain, Donostia International Physics Center, Paseo Manuel de Lardizabal 4, 20018 San Sebastián, Spain, , Jülich Centre for Neutron Science, Forschungszentrum Jülich GmbH, outstation at Heinz Maier-Leibnitz Zentrum, Lichtenbergstr.1, 85747 Garching, Germany, and Laboratory for Neutron Scattering, Paul Scherrer Institut, CH-5232 Villigen, Switzerland

E-mail: a.arbe@ehu.eus

[*]To whom correspondence should be addressed
[†]CFM(CSIC–UPV/EHU)/MPC
[‡]UPV/EHU
[¶]IKERBASQUE
[§]DIPC
[‖]Current address: Department of Physics and Astronomy, Wayne State University, Detroit, MI 48201, USA
[⊥]JCNS
[#]PSI

Abstract

We present Neutron Spin Echo (NSE) experiments on the single chain dynamic structure factor of long poly(ethylene oxide) (PEO) linear chains in the presence of poly(methyl methacrylate)-based single-chain nano-particles (SCNPs). A complementary structural characterization of the system discards a significant interpenetration of the components and reveals a close to globular conformation of the SCNPs when surrounded by PEO chains. Analogous NSE measurements on blends of PEO with the linear precursor chains of the SCNPs are taken as a reference for the dynamics study. For short times (below approx. 5 ns) PEO in both mixtures exhibits slowed down Rouse dynamics with respect to bulk PEO behavior. The similar deceleration observed in both environments suggests this effect to be due to the large dynamic asymmetry in the mixtures as evidenced by DSC experiments. More interestingly, the NSE results at longer times reveal a spectacular increase of the explored volume of PEO chains in the all-polymer nano-composite that is absent in the blend with linear precursor chains: assuming the reptation model, apparent tube diameter confining PEO chain motions in the nano-composite is about 80% larger than in bulk PEO. This can be considered as the first NSE direct observation of disentanglement in a nano-composite.

I. Introduction

Due to the macromolecular nature of their structural units, polymers exhibit a large variety of dynamical processes which relevance depends on the length scale of observation: vibrations and local relaxations dominate at small length scales; the structural relaxation universal for glass-forming systems is the leading process at intermolecular level and chain dynamics governed by entropy and macromolecular connectivity determines the large-scale motions. For unentangled chains and long chains at short times these ingredients are successfully captured by the Rouse model.[1–3] A key question in the field of polymer physics is to characterize and understand how polymer dynamics are affected by confinement. Interestingly enough, this situation naturally emerges already in a melt of sufficiently long polymeric chains. The uncrossability of macromolecules leads to topological constrains ('entanglements') that restrict laterally the chain motions. Such 'self-confinement' effect –responsible in fact for the singular viscoelastic character of polymers– is captured by the 'tube' concept invoked in the reptation model:[4] for long times, chain fluctuations take place within a fictitious tube of diameter d_{tube} parallel to the chain profile. Neutron scattering (in particular, neutron spin echo, NSE) experiments on labeled entangled polymeric samples, addressing the single chain dynamic structure factor $S_{chain}(Q,t)$, have provided the microscopic evidence for the existence of such confinement effects.[3] They manifest themselves as long-time plateaus in $S_{chain}(Q,t)$ from which d_{tube}-values can be directly extracted. These are of the order of 5 nm.

Superimposed to this inherent restriction, additional confinement effects may arise in more complex systems where polymeric chains are mixed with other entities –as it is the case of commonly end-use polymer-based materials, such as polymer blends or nano-composites. The latter are nowadays focus of great scientific interest, mainly due to their potential applications. Despite the efforts, the confinement effects induced by nano-particles on polymer motions are still far from being well understood. A specially intriguing question is: how do nano-particles affect the 'tube'? NSE experiments on a nano-composite where linear polymer chains were mixed with spherical silica nano-particles[5] revealed a decrease of the apparent

tube diameter, i. e., an enhancement of the lateral restrictions to chain motions. To explain the finally observed effect, the authors of that work invoked the simultaneous action of two mechanisms: on the one hand, the geometrical confinement due to interactions of the chains with the nano-particles and, on the other hand, the proper entanglements with the rest of the chains. Based on an estimation of the geometrical contribution, from the experimentally observed effective tube dimensions they extracted the diameter of the tube characterizing pure entanglements effects. From such an analysis, a somewhat counterintuitive *increase* of the diameter of the tube due to entanglements was deduced. It is worth emphasizing that entanglement tube dilation in confinement had been unambiguosly reported by NSE experiments on polymer chains under the well-defined confining geometry provided by cylindrical nanopores of anodic alumina oxide (AAO).[6] Seemingly, an analogous effect could be inferred for the case of the nano-composite with spherical silica nano-particles.[5] With increasing nano-particle-concentration ϕ, such dilution effect would become more important –but at the same time overwhelmed by the enhanced geometrical constraint by the nano-particles, finally leading to the experimental observation of a narrower tube with respect to bulk. Unfortunately, experimentally it is not possible to univocally unravel the two contributions to the tube. Nevertheless, a dilution of the entanglement network was later corroborated by molecular dynamics (MD) simulations on similar polymer/spherical-nano-particles nano-composites.[7] Conversely, macroscopic (mechanical) measurements on sterically stabilized silica-nano-particle nano-composites showed an increase of the confining tube diameter, which was attributed to a plasticization effect of the particle-tethered chains on the entangled polymeric matrix.[8] We note that compatibilization of nano-composite components is a difficult issue and the methods used to promote it may induce additional ingredients hampering the origin of the finally observed effects on chain dynamics. Thus, we can state that, as far as our knowledge, the *direct microscopic* evidence for entanglement dilution due to confinement effects in a *real nano-composite* still remains elusive.

Single-chain nano-particles (SCNPs) –nano-objects obtained by internal cross-linking of

individual linear macromolecules– are promising candidates to be mixed with linear polymers, leading to novel nano-composites with tunable properties. Particularly remarkable is the possibility of choosing miscible polymers for matrix and nano-particles, eliminating thereby compatibility problems. Interestingly, striking effects were reported by Mackay et al.[9] and Tuteja et al.[10] on all-polymer nano-composites based on polystyrene. Among others, a drastic decrease of the viscosity, suggesting this kind of nano-composites as potential systems to experimentally realize the definitive microscopic observation of entanglement dilution invoked in the literature.

Here we present a NSE investigation of the dynamics of long poly(ethylene oxide) (PEO) linear chains –which in the bulk are clearly entangled with $d_{tube}^{bulkPEO} = 5.3$ nm[11]– in an all-polymer nano-composite with SCNPs based on poly(methyl methacrylate) (PMMA). The chosen composition is 75wt%PEO/25wt%SCNPs. In parallel, we have studied the analogous linear blend system, where PEO is mixed with the linear precursors of the SCNPs. The weak (favorable) interaction between these two polymers[12] assures thermodynamic miscibility. We also recall that due to the huge difference in glass-transition temperatures of the two components, PMMA/PEO blends, mainly those rich in the PMMA component, have been subject of high interest since such mixtures present a large dynamic asymmetry.[13] Our study is complemented by a structural characterization by small angle neutron scattering (SANS) and wide angle X-ray scattering (WAXS) and differential scanning calorimetry (DSC) experiments.

After describing the experimental details, we first present the structural characterization, that discards a significant interpenetration of the components and reveals a highly compact conformation of the SCNPs when surrounded by PEO chains. The following described DSC results show a clear impact of the mixture on the glass-transition temperatures of both components in the nano-composite, in a similar way as in the linear blend counterpart. This observation could be attributed to the huge amount of interface provided by the ultra-small size of the SCNPs and points to a good dispersion of them in the nano-composite.

The DSC experiments also demonstrate the presence of two distinguishable glass-transition temperatures associated to each component in the mixtures, which is a signature of a strong dynamic asymmetry also in these systems rich in the PEO-component.

Thereafter, the analysis of the single chain dynamic structure factor of the PEO component in the mixtures obtained by NSE is presented. In the time range below approx. 5 ns, the results reveal very similar Rouse-like dynamics in both systems, which is clearly slowed down with respect to that observed in bulk PEO. The results on the Rouse dynamics are compared with those previously reported by some of us for the same nano-composite with the proper isotopic labeling to probe PEO hydrogen self-motions.[14] The similarity of the behavior at such short times of PEO dynamics in presence of nano-particles and linear precursor chains suggests attributing the observed slowing down to an increase of the friction for PEO chain motions due to the rigidity imposed by the effectively frozen PMMA-based component.

The NSE results at longer times reveal however a strikingly different evolution of the chain dynamic structure factor of PEO in both mixtures. In the linear blend, local reptation with very similar or hardly diluted entanglement network with respect to that reported for bulk PEO is found ($d_{tube}^{PEO/LB} \approx d_{tube}^{bulkPEO}$; LB: linear blend with precursor). On the contrary, we observe a dramatic release of the restrictions to PEO chain motions in the nano-composite. If the reptation model is assumed, the apparent tube diameter $d_{tube}^{PEO/NC}$ in the nano-composite (NC) is about 80% larger than $d_{tube}^{bulkPEO}$. This can be considered as the first NSE direct observation of tube dilation in a nano-composite. The spectacularity of the effects in the all-polymer nano-composite compared to other nano-composites is tentatively attributed to the huge amount of interfaces provided by the peculiar topology of SCNPs.

II. Experimental

The SCNPs were obtained through Michael addition-mediated multidirectional self-assembly of individual polymeric chains (precursors) at room temperature in tetrahydrofuran, by following the procedure reported in Ref.[15] As precursors, linear copolymers of methyl methacrylate (MMA) and (2-acetoacetoxy)ethyl methacrylate (AEMA) P($MMA_{0.63}$-co-$AEMA_{0.37}$) were used. Ethylene glycol diacrylate (90%, Sigma-Aldrich) acted as intrachain cross-linking agent. The estimated reacted fraction was about 0.4, corresponding to about 1 link / Kuhn length in average. The investigated nano-composite contained 25wt% of SCNPs. To achieve the needed contrast to follow PEO dynamics by neutron scattering, 10wt% of the sample consisted of protonated PEO chains (hPEO, $M_w = 94$ kDa, $M_w/M_n = 1.08$) while the rest of PEO (65wt%) was deuterated (dPEO, $M_w = 96$ kDa, $M_w/M_n = 1.08$) and the SCPNs ($M_w =$ 95 kDa, $M_w/M_n = 1.1$) were synthesized with deuterated MMA-monomers. The molecular weight of PEO is well above its entanglement mass in bulk ($M_e = 2.16$ Kg/mol[11,16]). Samples consisting of the same composition but with linear precursor chains instead of SCNPs were prepared and investigated in parallel.

For the determination of the SCNPs conformation in a PEO matrix, a sample where 4wt% protonated SCNPs ($M_w = 92$ kDa, $M_w/M_n = 1.07$) were dispersed in the above described dPEO chains was prepared. The SANS experiments were performed at the SANS-1 instrument at SINQ, Paul Scherrer Institute, Villigen (Switzerland). Using wavelength $\lambda = 6$ Å, the scattered intensity was recorded with sample-detector distances of 8 and 2 m. The temperature of the sample was 100°C, in the molten state of the dPEO-matrix. The short-range order of the nano-composite with 25wt% SCNPs was investigated by WAXS on a Rigaku equipment with a two-dimensional multiwire X-Ray Detector. Measurements were performed in transmission geometry, with the film fixed perpendicular to the beam at a distance of 24 cm from the detector. The temperature was also 100°C.

A differential scanning calorimeter TA Instrument Q2000 was used to measure the calorimetric glass transition temperature of the samples. Modulated Differential Scanning Calorime-

try (MDSC) allows to separate changes in the heat flow due to variations in the heat capacity (C_p) of the sample from other type of heat contributions, that is, the so called reversible and non-reversible contributions. Samples of about 10 mg were sealed in aluminum pans and cooled from 423 K at an average 3 K/min rate with temperature modulation amplitude and period of ± 0.5 K and 60 s respectively. The reversible part of the heat flow reveals then the glass-transition processes free from crystallization signatures. Heating the sample at the same rate, from the total heat flow the melting temperatures were deduced.

Neutron Spin Echo (NSE) provides the highest resolution achievable by neutron scattering methods. NSE experiments were performed at $T = 435$ K by the JNSE instrument at the Forschungs-Neutronenquelle Heinz Maier-Leibnitz in Garching. Using two wavelengths (8 and 10 Å), Fourier times in the range $0.1 \leq t \leq 70$ ns were covered for three momentum transfer (Q)-values: 1, 1.3 and 2 nm^{-1}. The data were corrected for the matrix contribution by subtracting the background signal measured on the fully deuterated samples with equal statistics as for the labelled samples.

In general, the measured NSE signal is given by[3,17]

$$\tilde{S}_{NSE}(Q,t) = \frac{I_{coh}\tilde{S}_{coh}(Q,t) - \frac{1}{3}I_{inc}\tilde{S}_{inc}(Q,t)}{I_{coh} - \frac{1}{3}I_{inc}} \tag{1}$$

where $\tilde{S}_{coh}(Q,t)$ and $\tilde{S}_{inc}(Q,t)$ are the normalized coherent and incoherent intermediate scattering functions and I_{coh} and I_{inc} represent the coherent and incoherent differential cross sections respectively. Measurements performed in diffraction mode showed that the coherent contribution to the NSE signal in our samples (I_{coh}) is dominant as compared to that of incoherent nature ($-I_{inc}/3$), as can be seen in Fig. 1. On labelled samples like those investigated in this work and in the low-Q range here considered, the coherent differential cross section reflects the single chain structure factor. Therefore, the ratio in Fig. 1 is amplified with decreasing Q-value and the obtained NSE signal directly reveals, to a good approximation, the normalized single chain dynamic structure factor $S_{chain}(Q,t)/S_{chain}(Q,0)$.

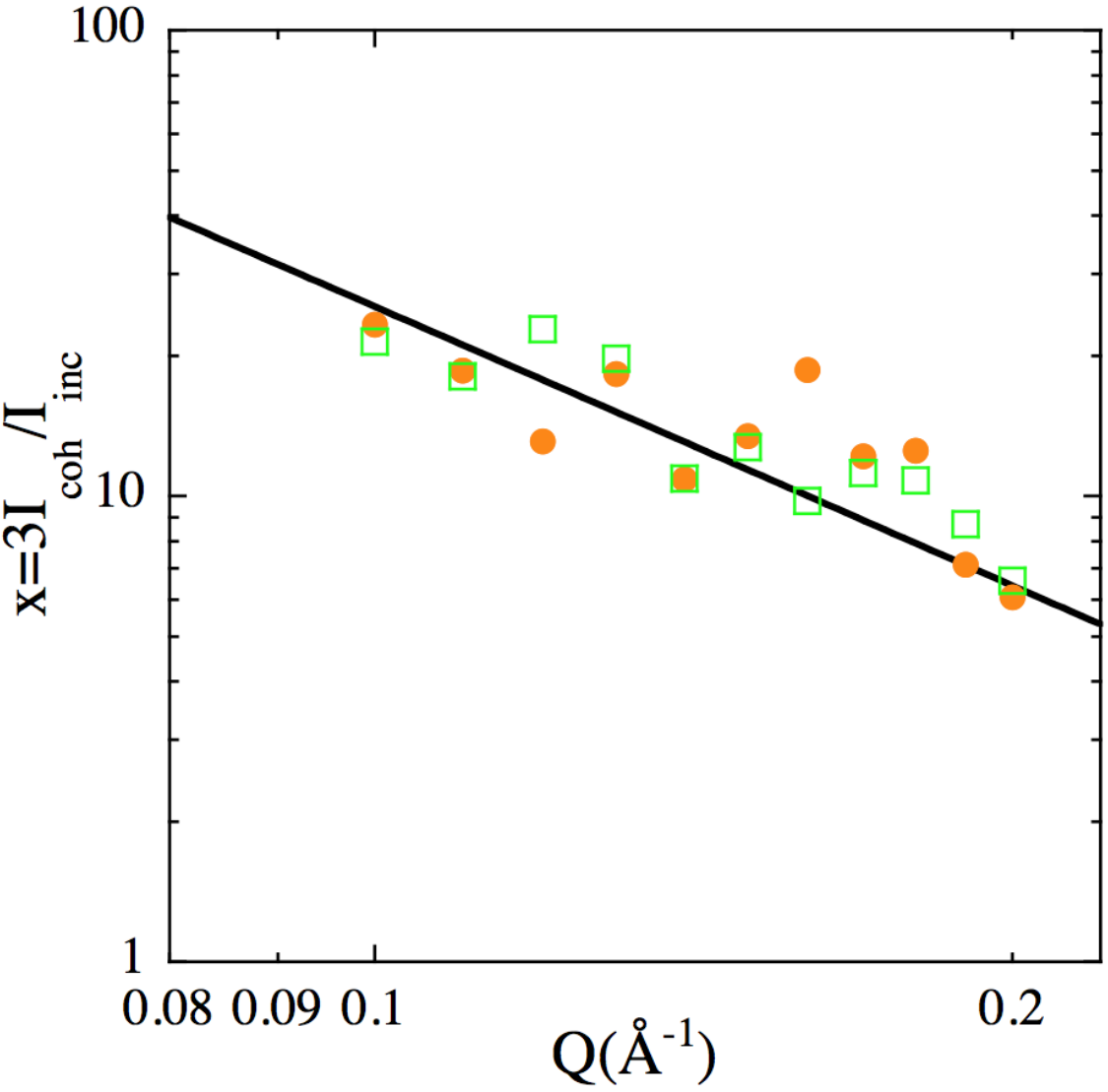

Figure 1: Momentum transfer dependence of the absolute value of the ratio between the coherent and the incoherent contributions to the NSE signal of the nano-composite sample (filled circles) and the blend with the precursor (empty squares). The coherent contribution is at least 6-fold higher than the incoherent one. Solid line shows a Q^{-2}-power law.

III. Results and Discussion

A. Structural Features

A crucial question regarding the structural features (and with clear potential impact in the dynamical behavior) of the nano-composite is whether there is an interpenetration of the two components. To address it we first consider the information on the short-range order provided by the WAXS experiments. Figure 2 shows the results for the nano-composite as empty squares. The data reported in Ref.[18] for the neat components at the same temperature are also included in the figure. In the Q-range explored, the patterns reveal broad maxima of the structure factor. The unique peak of bulk PEO centered at about 1.37 Å^{-1} can be interpreted as due to inter-main chain correlations with associated average distances of about $d_{chain} = 2\pi/Q_{max} \approx 4.6$ Å. Deciphering the origin of the correlations leading to the peaks in the patterns of the melt of SCNPs would require the help of molecular dynamics simulations and is beyond the scope of this work, but it can be expected that the contributions involving nearest neighbor chain segments show up in the Q-range explored by WAXS. Here we use these results just to look for signatures of interpenetration of the components in the nano-mixture. If the components are not mixed at monomer level, the measured pattern would be simply given by the weighed addition of the individual structure factors corresponding to the pure components. On the contrary, if they are interpenetrated, in the WAXS Q-range we would expect additional contributions of cross-correlation terms involving pairs of atoms of PEO and SCNPs to the structure factor of the mixture. The simple concentration-weighted addition of the two individual structure factors of the neat components is represented by the solid line in Fig. 2. The experimental results on the nano-composite are very close to the such built pattern. Thus, the WAXS results strongly support the idea that the two components are not mixed at monomer level, i. e., the picture of a 'true' nano-composite, where PEO chains surround the nano-particles but do not deeply penetrate them.

This scenario is also confirmed by the SANS experiments. Figure 3 shows a Kratky-plot

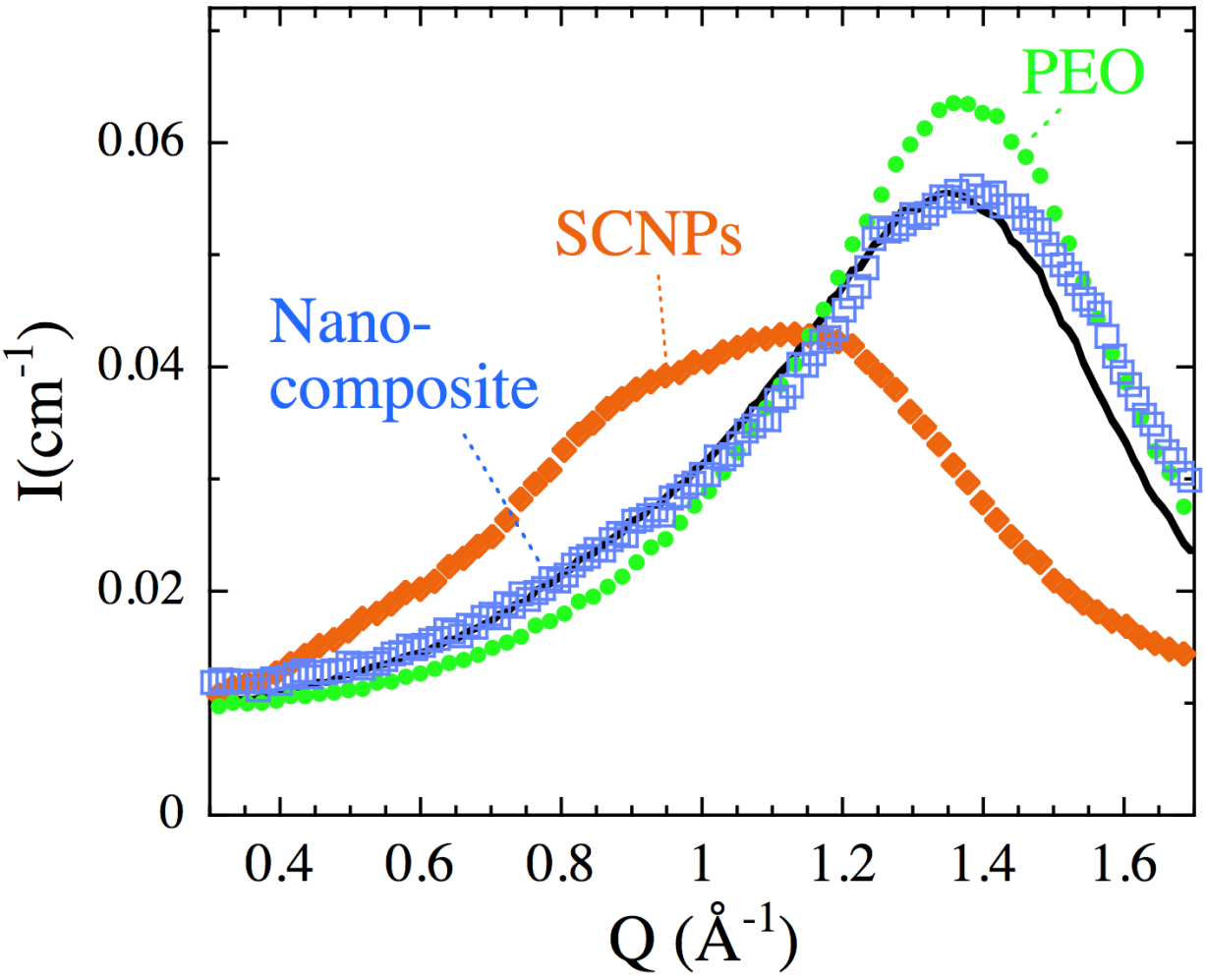

Figure 2: WAXS patterns obtained at 100°C for PEO (circles),[14] the SCNPs (diamonds)[14] and the nano-composite (squares). Solid line represents the result of combining the patterns corresponding to the neat components weighed by the respective volume fractions in the mixture.

of the SANS results revealing the macromolecular form factor of the SCNPs in the PEO matrix. The clear maximum displayed by the data is a signature of the high compaction degree of the SCNPs in this environment. Nowadays, it is well established that in solution, SCNPs obtained through cross-linking routes as those employed in this case adopt a sparse morphology.[15,19–23] Obviously, this conformation is dramatically changed in the nano-composite. In a first approximation, the data can be described by the form factor of a compact globule (completely collapsed coil). This function is given by a generalized Gaussian coil function[24]

$$P(Q) = \frac{1}{\nu U^{\frac{1}{2\nu}}}\gamma\left(\frac{1}{2\nu}, U\right) - \frac{1}{\nu U^{\frac{1}{\nu}}}\gamma\left(\frac{1}{\nu}, U\right) \tag{2}$$

$[U = (2\nu+1)(2\nu+2)Q^2\langle R_g^2\rangle/6;\ \gamma(a,x) = \int_0^x t^{a-1}\exp(-t)\mathrm{d}t]$ with scaling exponent $\nu = 1/3$. With this kind of description, a value of 5.5 nm is obtained for the radius of gyration $\langle R_g\rangle$ of the SCNP. We note that the scaling exponent in the fractal regime is thus close to 1/3 (rather different to the 1/4 value corresponding to a sharp interface), i. e., indicative for a crumpled or diffuse interface. In fact, a recent investigation of the structure of SCNPs in increasingly crowded environments by SANS experiments and coarse-grained molecular dynamics simulations[25] has shown that the actual structure of SCNPs in bulk systems like that here investigated is a *crumpled globule*-like[26] conformation. The simulations show a high polydispersity of topologies for the SCNPs, presenting protrusions toward the surrounding macromolecules and thus offering a large amount of interfacial area.

Regarding the PEO component, as commented above, the NSE diffraction data (Fig. 1) are determined by its chain form factor. In the Q-range covered by the NSE measurements the fractal regime is explored (intensity proportional to $Q^{-1/\nu}$), revealing a value of the scaling exponent compatible with that corresponding to a Gaussian coil $\nu = 1/2$. Unfortunately, the NSE results do not allow determining the size of the PEO chains within the nano-composite; we recall that for the molecular weight investigated the unperturbed radius of gyration of PEO chains is $\langle R_g^{bulkPEO}\rangle \approx 11.2$ nm.[27]

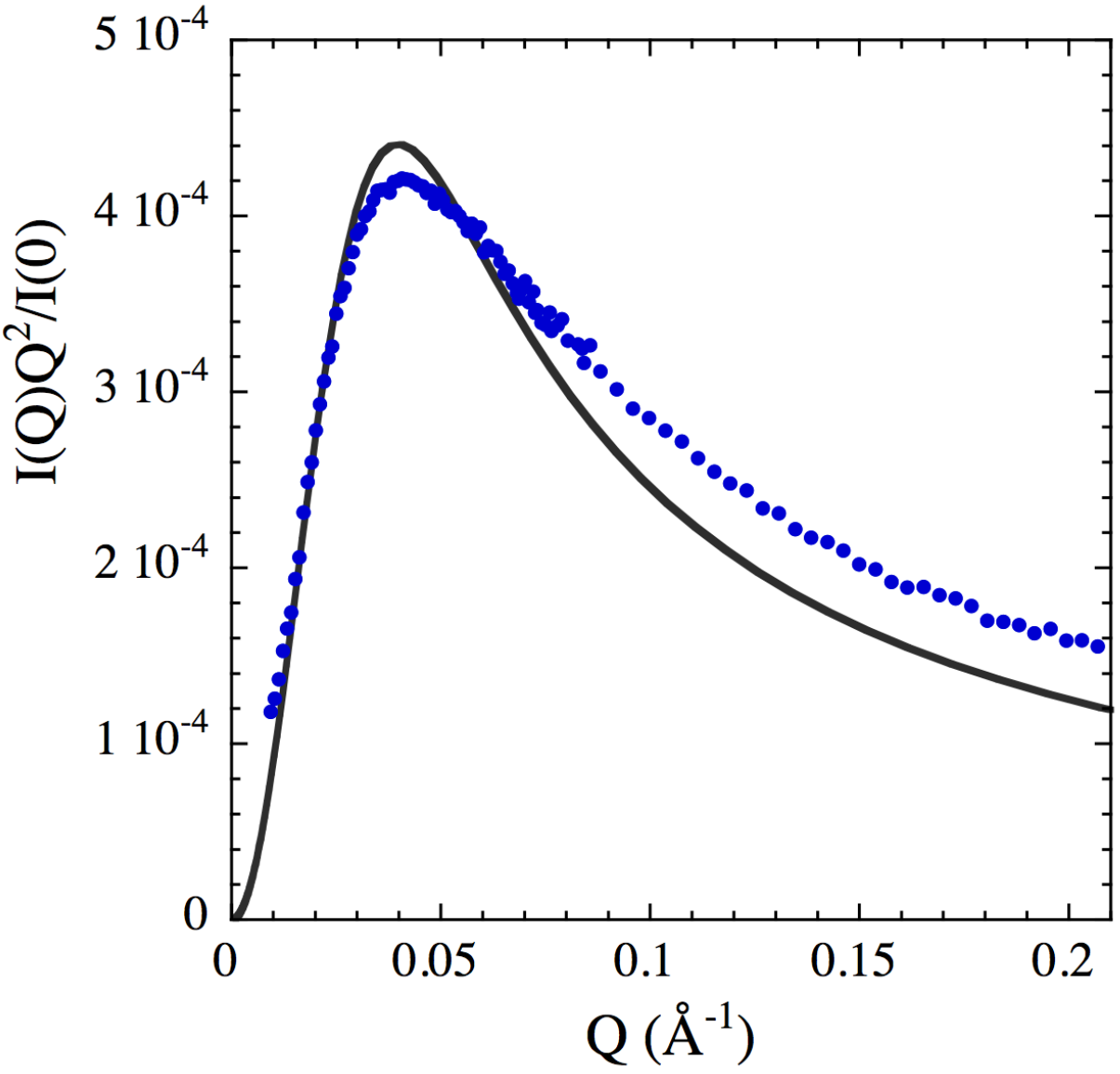

Figure 3: Kratky plot of the SANS results on the SCNPs form factor in a PEO matrix. Solid line is a fit of a collapsed globule form factor with scaling exponent $\nu = 1/3$ (Eq. 2), delivering a radius of gyration of 5.5 nm.

B. Glass Transitions and Dynamic Asymmetry

The temperature derivative of the specific heat provides a sensitive method to identify glass-transitions in complex systems –the location of a maximum in this function corresponds to the inflection point in the specific heat which is associated to a given glass-transition process. The results obtained are represented in Fig. 4 for the linear blend with the precursor [Fig. 4(a)] and the nano-composite [Fig. 4(b)]. The figures also show the results on the respective pure components.

The neat systems display a single clear glass-transition. Fits of a Gaussian $\propto \exp[-(T-T_g)^2/(2(\Delta T_g)^2)]$ to the peak –plus a flat background– deliver the values of the glass-transition temperature T_g and its width ΔT_g collected in Table 1. The glass-transitions of precursor and nano-particles differ by about 15 K due to internal cross-linking and both are sensitively lower than that of PMMA (400 K). This effect should be attributed to the internal plasticization of the polymer produced by the AEMA monomers. Even so, there is still a large difference between the T_g-values of the two pure components (around 97 and 112 K for the linear blend and nano-composite, respectively). The results on the mixtures evidence the presence of two distinct processes. Assuming two Gaussian components the data are rather well described, as shown in the figure. These contributions would be attributed to the 'effective glass-transitions' of each of the components in the mixtures: the Gaussian centered at lower temperatures would correspond to the glass-transition of PEO in the system and that at higher temperature to the slow component. The values deduced in this way for the effective glass transition temperature $T_{g,eff}$ and width of each component in the mixed systems are also listed in Table 1. These results reveal similar differences between the effective glass-transitions of the two components (about 55 K) for both the mixtures. This implies the presence of a clear dynamic heterogeneity: the segmental dynamics of PEO component is much faster than that of the PMMA-based component. Dynamic heterogeneity would intuitively be expected in a nano-composite, where the components are not mixed at monomeric level. Not so obvious could be this finding in miscible blends of linear polymer chains, where

mixing is assumed to reach the monomer length scale. In fact, a single glass-transition process was *traditionally* considered as the fingerprint of thermodynamic miscibility. However, the presence of two glass-transition temperatures in binary mixtures has been reported for a variety of miscible polymer blends (see, e. g., Refs.,[28–31] including the PEO/PMMA blend[32]) and nowadays is a well established experimental fact.[13] The self-concentration concept[33–35] has been put forward in order to rationalize such behavior. Conversely, we note that, at the same time, the effective vitrification temperatures of both components vary in the mixtures with respect to those in bulk. Such effect would be expected in the blend with components mixed at monomer level, but not *a priori* in a nano-composite. As we have demonstrated with the structural analysis, the interpenetration degree of the components, if any, has to be very small. However, we have to take into account that due to the ultra-small size of the SCNPs –their radius of gyration is only $\langle R_g \rangle \approx 5.5$ nm– there is a huge amount of interface between the two components. All those SCNPs segments at the interfaces will be in contact with much more mobile PEO segments and are expected to experience a plasticization effect. Conversely, PEO segments close to the SCNPs will feel the presence of a slower neighbor. Thus, the finding of mutual influence in the dynamics can be rationalized –at least qualitatively– invoking the important role of interfaces in the system and could also be considered as a signature of the good dispersion of the SCNPs in the nano-composite. Finally, we note the clear broadening of the glass transitions in the mixtures with respect to those in the neat components (see Fig. 4 and Table 1). In polymer blends, this effect is usually explained as a consequence of the thermally driven concentration fluctuations which are always present in a two-component system in equilibrium[36–43] In the nano-composite, the glass transition processs are even broader than in the linear blend with the precursor. This feature could be understand as a result of two ingredients: (i) particularly strong concentration fluctuations –due to the impenetrability of the SCNPs by the PEO chains above demonstrated, and bearing in mind that they are deformable– and (ii) the topological polidispersity exhibited by the SCNPs.[25]

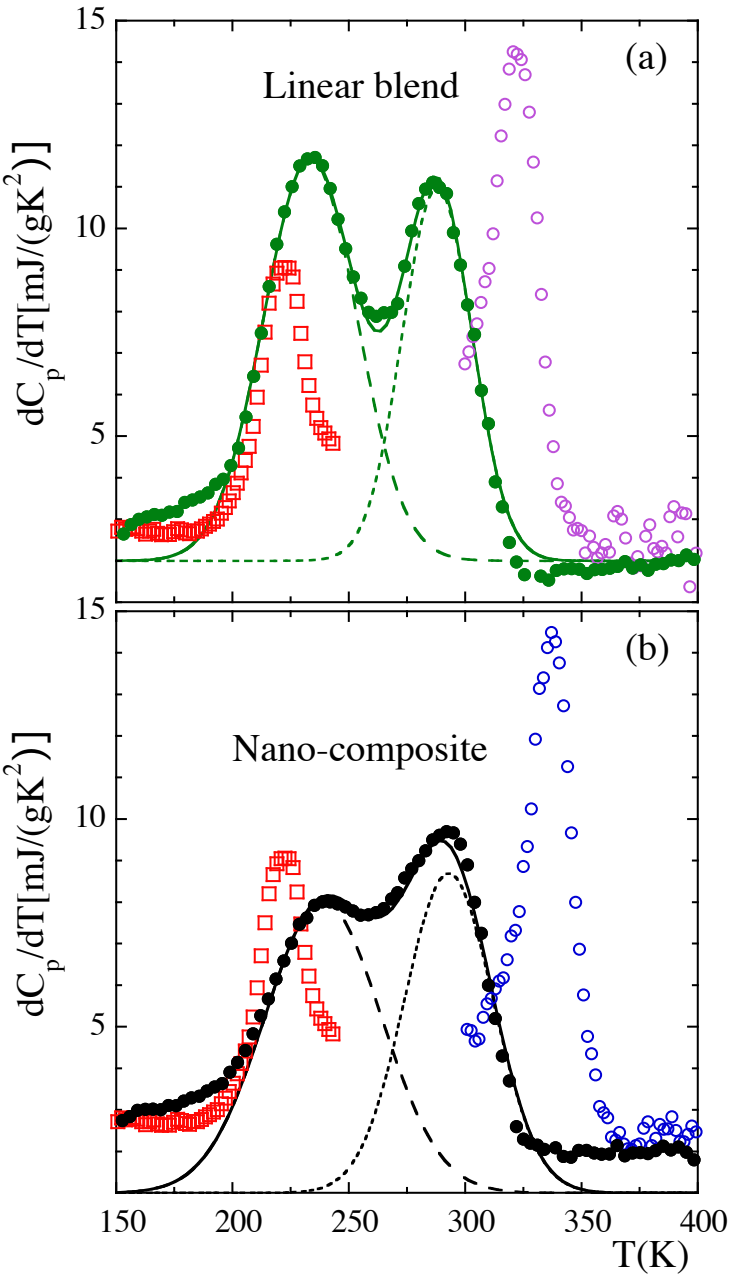

Figure 4: Temperature dependence of the derivative of the reversible heat flow with respect to temperature obtained by MDSC in the mixtures and their components: (a) the linear-blend system; (b) the nano-composite. Empty squares: bulk PEO; empty circles: bulk precursors in (a) and bulk SCNPs in (b); solid circles: linear blend in (a) and nano-composite in (b). Solid lines are fits of the sum of two Gaussians (depicted with the dashed and dotted lines) and a constant to the data of the mixtures.

Table 1: Melting temperature, glass transition temperature and width (maximum position and variance of the Gaussian fit of the heat-flow derivative) of the neat systems and the components involved in the mixtures (*other*: Precursor, SCNP).

Sample	T_M (K)	T_g (K)	ΔT_g (K)	$T_{g,eff}^{PEO}$ (K)	$\Delta T_{g,eff}^{PEO}$ (K)	$T_{g,eff}^{other}$ (K)	$\Delta T_{g,eff}^{other}$ (K)
*h*PEO	344	223	12				
*d*PEO	337	224	12				
Precursor		320	11				
SCNP		335	11				
Linear blend	328			233	20	288	15
Nano-composite	327			239	25	293	19

C. Single Chain Dynamic Structure Factor

The NSE results, revealing the normalized $S_{chain}(Q,t)$ of PEO, are presented in Fig. 5 with the abscissa in logarithmic scale to highlight the short times. For comparison, the lines show the theoretical (Rouse) curves describing the behavior of short unentangled chains of PEO in the bulk at the same temperature and Q-values. The Rouse model[1] describes the melt chain dynamics considering the conformational entropy as the only source for restoring forces which stabilizes excursions from equilibrium. The contribution of the surrounding chains is introduced as a stochastic background creating also a friction –characterized by the friction coefficient ξ– on each segment of length ℓ.[1,2] The main variable is the Rouse rate W, determined by the balance between the entropic forces and the friction $W = 3k_BT/(\ell^2\xi)$. At the temperature here investigated, the reported value for the Rouse variable $W\ell^4$ of bulk PEO is $W\ell^4 = 24150$ Å^4/ns.[11] Using this value, the Rouse curves shown in Fig. 5 have been constructed. As it was shown in Ref.,[11] long PEO chains in the bulk follow Rouse dynamics up to about 10 ns (represented by the dashed parts of the curves in Fig. 5). Due to entanglements with the surrounding PEO chains, deviations occur at longer times –the experimental $S_{chain}(Q,t)/S_{chain}(Q,0)$ of long PEO chains in bulk decays more moderately than the expected Rouse functions represented by the dotted parts of the curves in Fig. 5. The deviations from Rouse behavior of bulk PEO above ≈ 10 ns are successfully accounted for by the above mentioned tube model.[2] This model considers two relaxation mechanisms:

(i) local reptation –Rouse-like motion restricted to one dimension along the tube profile– and (ii) escape from the tube. The relaxation time of the latter process ('reptation time') becomes about 2 ms for the here considered molecular weight, i. e., far beyond the NSE experimental window. Then,

$$\frac{S_{chain}(Q,t)}{S_{chain}(Q,0)} = [1 - F(Q)]\, S^{loc}(Q,t) + F(Q) \ , \tag{3}$$

where $S^{loc}(Q,t)$ expresses the time-dependence of the contributions from the local (Rouse-like) motion

$$S^{loc}(Q,t) = \exp\left(\frac{W\ell^4}{36}Q^4 t\right) erfc\left(\frac{Q^2}{6}\sqrt{W\ell^4 t}\right) \ , \tag{4}$$

and the (cross-sectional) form-factor of the tube

$$F(Q) = \exp\left(-\frac{Q^2 d_{tube}^2}{36}\right) \tag{5}$$

is determined by the tube diameter d_{tube} characterizing the entanglement-induced confinement effects. For bulk PEO, $d_{tube}^{bulkPEO} = 5.3$ nm was reported in Ref.[11]

As can be appreciated in Fig. 5, in the whole time window investigated the dynamic structure factor of PEO in both mixtures (nano-composite and linear blend) seems to display a slower decay than unentangled bulk PEO. It is also noteworthy that for long times above about 10 ns, the differences with respect to unperturbed bulk PEO dynamics become markedly more pronounced in the linear blend than in the nano-composite.

1. Rouse Dynamics

As pointed out above, PEO chain dynamics is altered by the presence of either precursor chains or SCNPs already from very short times. This means that the Rouse dynamics is affected in the mixtures and therefore a different value of the Rouse variable with respect to that in bulk is expected to be found in our systems. To determine this value, we have

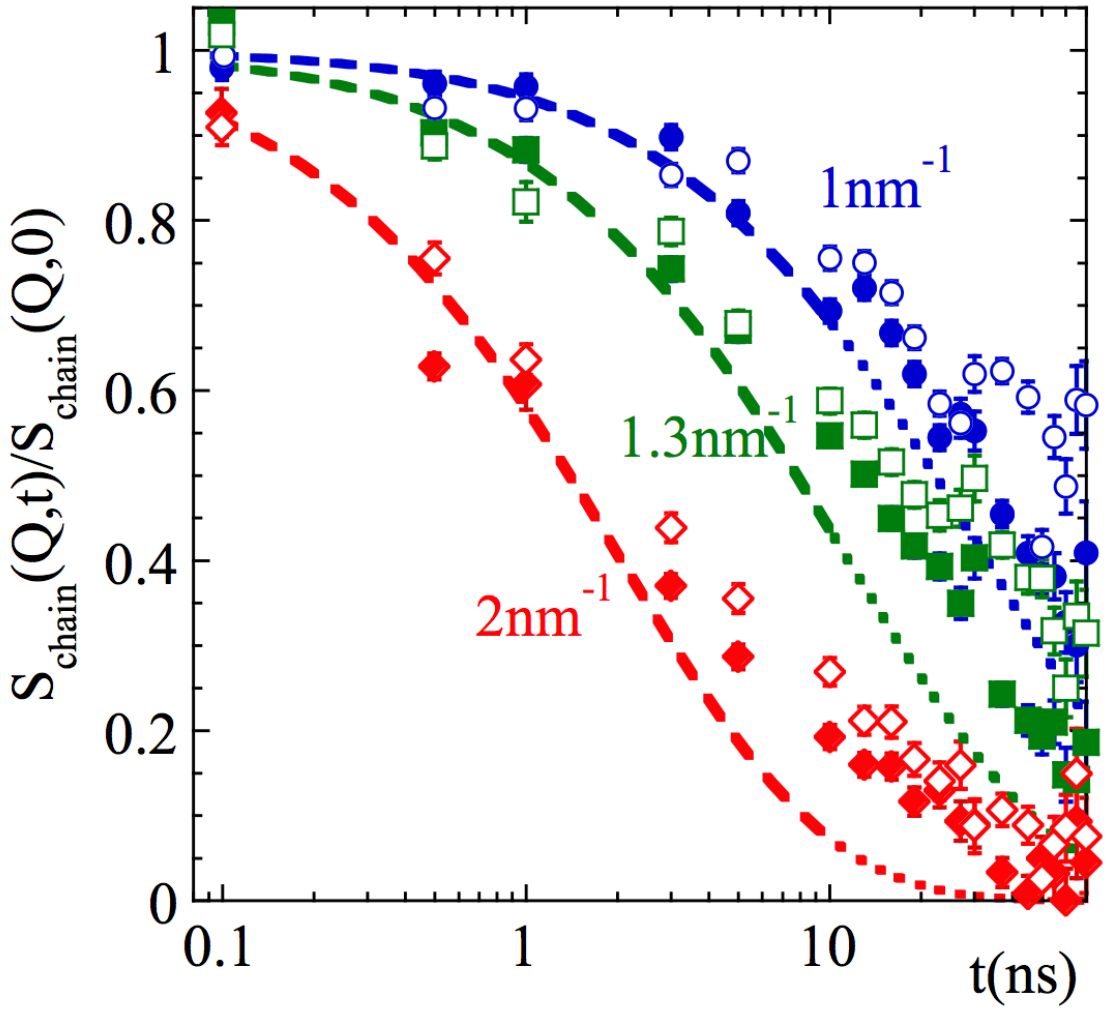

Figure 5: Normalized $S_{chain}(Q,t)$ of PEO chains in the nano-composite with SCNPs (filled symbols) and in the linear blend (empty symbols) at $Q = 1$ nm^{-1} (circles), 1.3 nm^{-1} (squares) and 2 nm^{-1} (diamonds). The abscissa (time) is represented in logarithmic scale. Lines display the Rouse description of bulk-PEO behavior at the same temperature ($W\ell^4 = 24150$ Å^4/ns), which for entangled chains is followed up to 10 ns.[11]

fitted the Rouse model to the initial decay ($t \leq 5$ ns) of the PEO single chain dynamic structure factor in the nano-composite measured by NSE. With $W\ell^4 = 17000$ Å^4/ns, this model provides a nice description of the data, as can be seen in Fig. 6(a). This value of the Rouse variable is clearly smaller than that reported for bulk PEO at the same temperature (24150 Å^4/ns[11]), that has been used to build the theoretical curves in Fig. 5.

In a recent study[14] a sample where protonated PEO chains were mixed with deuterated SCNPs with the same concentration as in this work was investigated by backscattering and time-of-flight techniques. The measured quasielastic scattering thus revealed the incoherent scattering function of PEO hydrogens in the temperature range 350 K $\leq T \leq$ 400 K and Q-range $0.5 \leq Q \leq 1.8$ Å^{-1}. The Fourier Transform of this function to the time domain was fitted by a stretched exponential $S_{inc}(Q,t) \approx \exp[-(t/\tau_{inc}(Q))^{\beta}]$ with values of the stretching exponent β close to 0.5. Such time-dependence is that expected for the incoherent scattering function corresponding to Rouse dynamics $S_{inc}^{Rouse}(Q,t) = \exp[-(\sqrt{W\ell^4/9\pi}Q^2t^{1/2})]$. Thus, from the Q-dependent characteristic time $\tau_{inc}(Q)$ an effective Rouse variable was obtained as $(W\ell^4)_{eff}(Q) = 9\pi Q^{-4}/\tau^{inc}(Q)$. The such deduced $(W\ell^4)_{eff}(Q)$ are reproduced in Fig. 7, together with the results reported for bulk PEO from similar experiments and molecular dynamics simulations.[44] This comparison also evidences that the presence of SCNPs induces a slowing down of PEO dynamics as monitored by H-self motions, at lower temperatures and more local length scales as those explored in the present study. Approaching the lowest Q-values accessed by those experiments, $W\ell_{eff}^4(Q)$ exhibits a Q-independent behavior, suggesting that the observed dynamics obeys the Rouse model in that range. At high Q, as expected, the model fails; there, its simplifying assumptions cease to be valid and the microscopic details come into play. Ingredients like chain stiffness, rotational potentials, local relaxations across the rotational barriers leading to an internal viscosity emerge at short length scales.[1,3,45] The particular mechanisms leading to deviations from pure Rouse behavior for bulk PEO were investigated in the light of molecular dynamics simulations.[44] Chain stiffness and internal friction were identified as their main sources. These combined

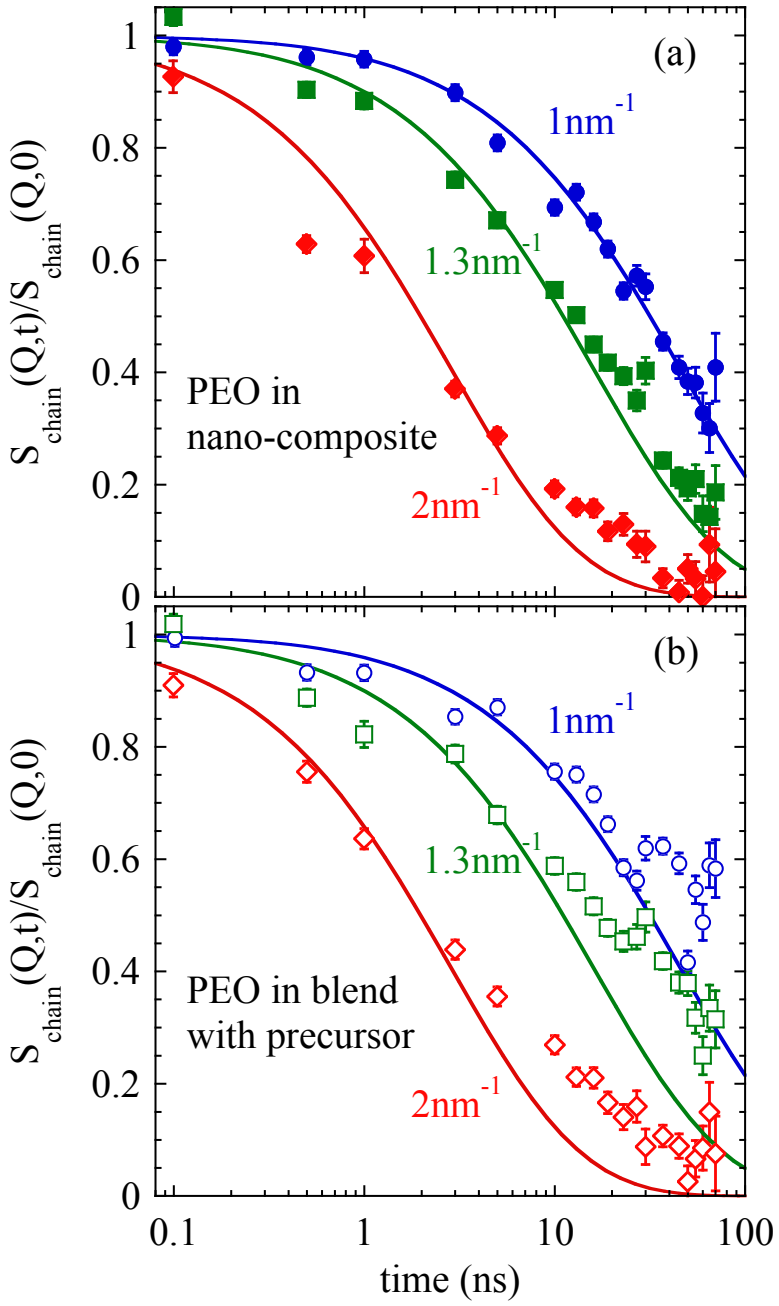

Figure 6: Normalized $S_{chain}(Q,t)$ of PEO chains in (a) the nano-composite and (b) the linear blend at the Q-values indicated. Solid lines are descriptions with the Rouse model ($W\ell^4 = 17000$ Å^4/ns).

mechanisms would be present in the nano-composite as well; in this case, non-Gaussian effects arising from the discrete nature of the elementary processes underlying the subdiffusive dynamics in the polymer were also suggested to have potential importance in determining the dynamical behavior at high Q.[14] Having said this, the presence of the low-Q plateaus is consistent with the Rouse model beyond a given length scale and allows the determination of the values of $W\ell^4$ from the asymptotic low-Q limits of the results. The such obtained $W\ell^4$-values for the nano-composite are shown in Fig. 8 as filled circles. They compare very well with the result from this NSE investigation (filled triangle). The figure also includes the $W\ell^4$-values reported in the literature for bulk PEO (empty symbols). The temperature dependence of the data can be described by Vogel-Fulcher laws

$$W\ell^4 = (W\ell^4)_\infty \exp\left[-\frac{B}{T-T_o}\right]. \tag{6}$$

The line through the bulk data in Fig. 8 represents the reported law in Ref.,[44] with $(W\ell^4)_\infty^{bulkPEO} = 1.18 \times 10^6$ Å^4/ns, $B^{bulkPEO} = 1090$ K and $T_o^{bulkPEO} = 155$ K. To describe the results in the nano-composite we have fixed the $B^{PEO/NC}$-value to that for bulk PEO and made an estimation of $T_o^{PEO/NC}$ on the basis of the calorimetric results. Namely, we have assumed that the shift observed by DSC for the values of the glass-transition temperatures of bulk PEO and PEO in the nano-composite (about 16 K, see Table 1) is also reflected in this Vogel temperature. This leads to $T_o^{PEO/NC} = T_o^{bulkPEO} + 16$ K $= 171$ K. As can be seen in Fig. 8, the obtained curve describes very well the data allowing for a slightly smaller value of the prefactor than in bulk [$(W\ell^4)_\infty^{PEO/NC} = 8.5 \times 10^5$ Å^4/ns]. We thus find a highly consistent description of the PEO results in the nano-composite obtained through different techniques.

Interestingly enough, just the same value of the Rouse variable fitting the NSE results of PEO in the nano-composite provides an excellent description of the single chain dynamic structure factor of PEO in the linear blend with the precursor at times below approx. 5 ns [see Fig. 6(b)]. This observation is in agreement with the rather similar shifts in glass-transition

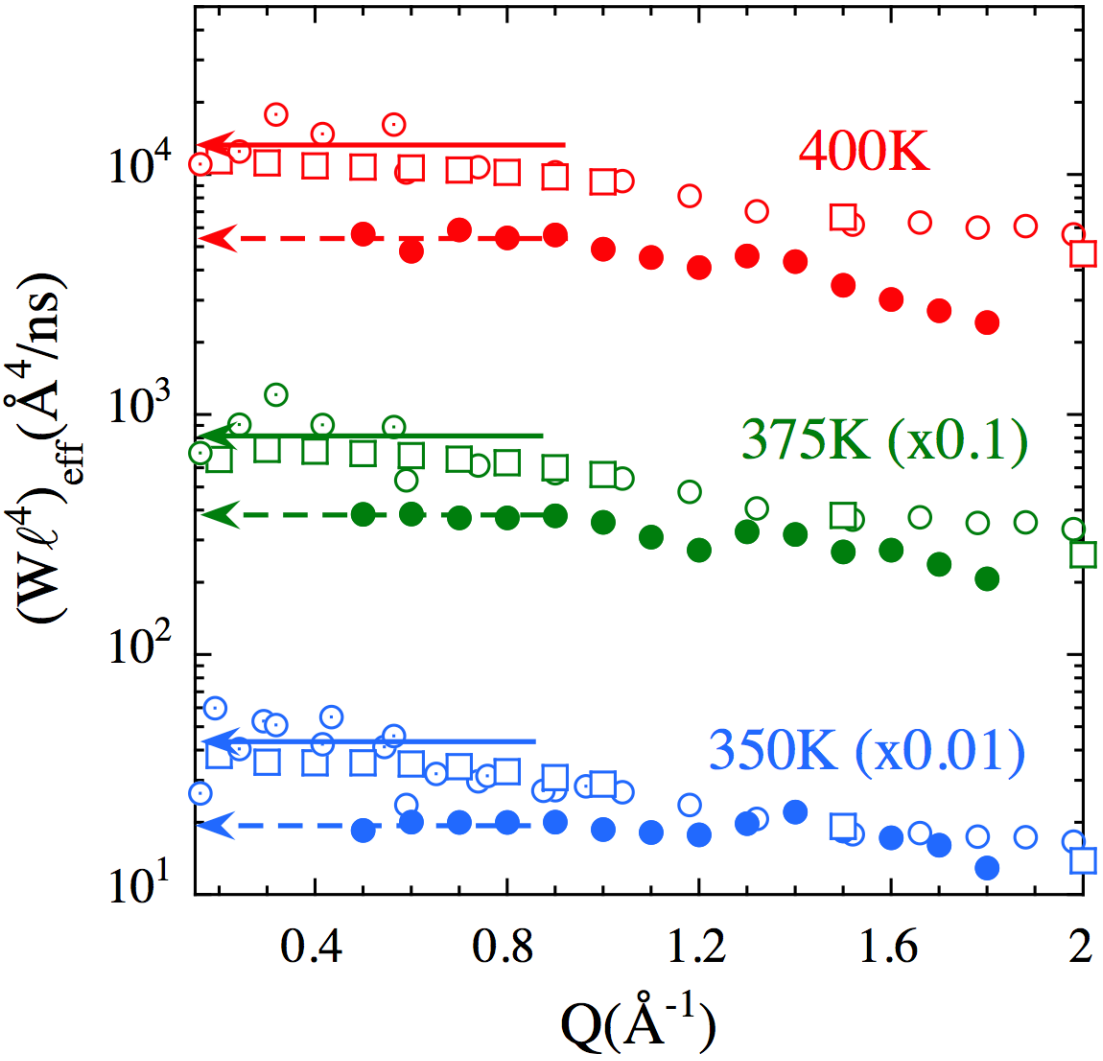

Figure 7: Momentum transfer dependence of the effective Rouse variable obtained in Ref.[14] from the incoherent scattering function of PEO in the nano-composite (filled circles) compared with the analogous results for bulk PEO (empty symbols) from time of flight (circles), backscattering (circles with dot) and MD-simulations (squares). Results at 375 K and 350 K have been divided by 10 and 100 for clarity. Dashed arrows show the low-Q asymptotic limit for the nano-composite data, and solid arrows the values for bulk PEO corresponding to the VF description shown in Fig. 8.

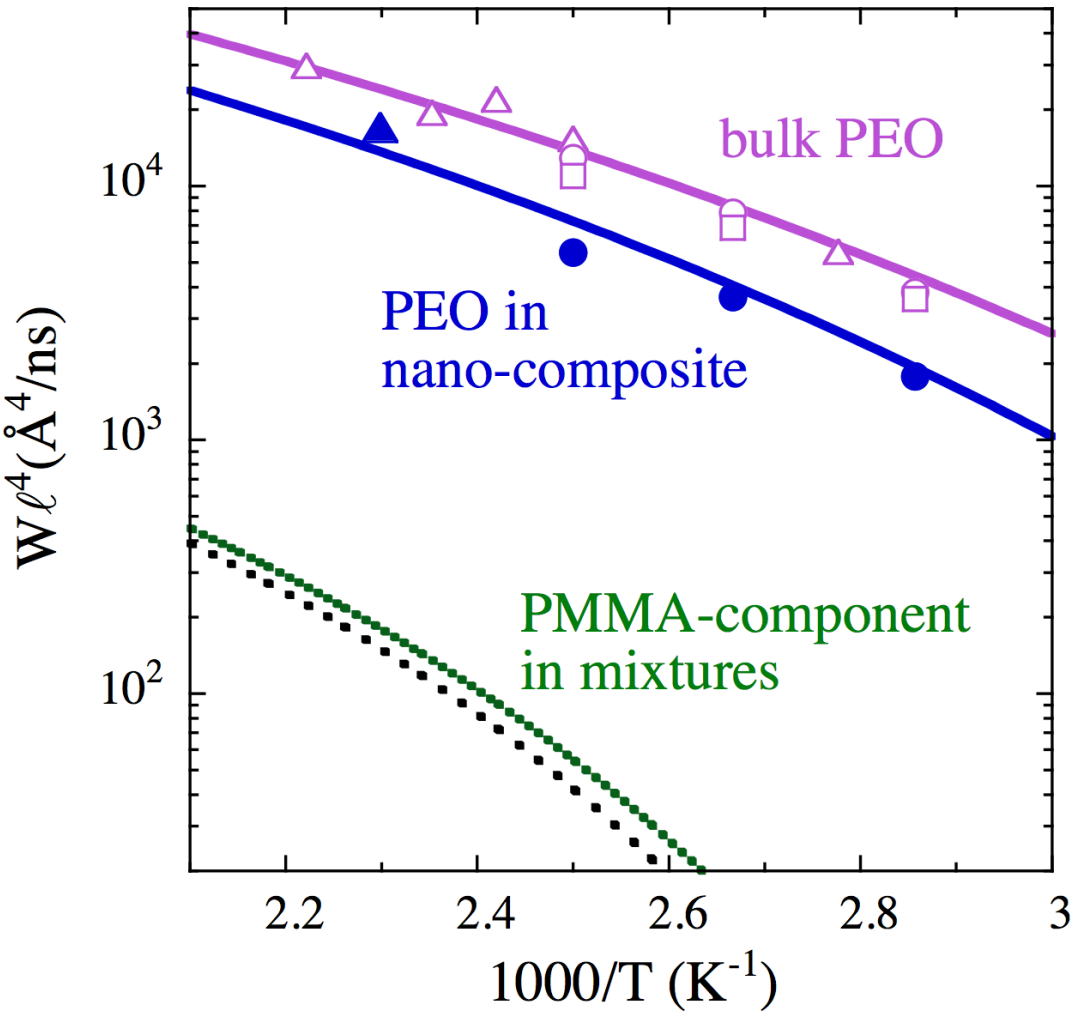

Figure 8: Inverse-temperature dependence of the Rouse variable reported from incoherent scattering (circles: experiments; squares: MD-simulations) and NSE experiments on the single chain dynamic structure factor (triangles) for bulk PEO[11,44] and for PEO in the nano-composite (from Ref.[14] and this work). Lines are VF laws: solid lines are fits to the PEO sets of data and dotted lines the expectations for the PMMA component of the mixtures [green: precursor; black: SCNP ('equivalent'-$W\ell^4$)] (see the text).

temperatures found by calorimetry for PEO in both samples (see Fig. 4 and Table 1).

Both, SCNPs and linear precursor, are based on PMMA, and, as demonstrated by DSC, display a much higher effective glass transition temperature than PEO in the mixtures. We may estimate the range of Rouse-like characteristic frequencies expected for the PMMA-like components in the mixtures at the high temperatures explored by neutron scattering techniques. We start considering the backscattering data reported in Ref.[46] for bulk PMMA at 518 K, revealing main-chain and α-methyl group hydrogen dynamics. Those results were characterized by a stretched exponential for the intermediate scattering function with $\beta = 0.5$ and $\tau^{inc}(Q) \propto Q^{-4}$ for $Q < 0.7$ Å^{-1} approximately, suggesting thus a crosover toward Rouse dynamics in such regime. Following the same reasoning as above for the PEO component, from the low-Q limit of the reported characteristic time $\tau^{inc}(Q)$ we can deduce $W\ell^4 = 9\pi Q^{-4}/\tau^{inc}_{lowQ} \approx 70$ Å^4/ns. Conversely, the temperature dependence of PMMA segmental dynamics is described by a VF law with $B^{bulkPMMA} = 843$ K and $T_o^{bulkPMMA} = 371$ K.[47] This implies a prefactor $(W\ell^4)^{bulkPMMA}_{\infty} = 2.17 \times 10^4$ Å^4/ns to satisfy $W\ell^4(518\text{ K}) = 70$ Å^4/ns. Now based on this description of the bulk PMMA $W\ell^4$ parameter, we estimate the corresponding values for the linear precursor in the blend. As a first approach, we keep in Eq. 6 the prefactor and the B-value as those for bulk PMMA. The T_o-value might be shifted according to the DSC result for the precursor component in the mixture shown in Table 1 ($T_{g,eff}^{Precursor/LB} = 288$ K). Taking into account that $T_g^{bulkPMMA} = 400$ K, the shift in glass-transition temperature is then of 112 K. Considering the T_o-value for bulk PMMA and this shift, we arrive at $T_o^{Precursor/LB} = 259$ K. The such calculated curve is represented in Fig. 8 as the dotted green line. These data show a difference in about two orders of magnitude with respect to the PEO component NSE results. Even if the uncertainties might be large and the assumptions involved in these calculations are quite strong, we can state that the chain dynamics of the precursor are expected to be effectively frozen with respect to PEO motions, even at the high temperature here investigated.

Regarding the SCNPs, they are also of macromolecular origin and consequently display

internal dynamics as well. This dynamics is probably distorted with respect to that occurring in the equivalent linear chain, and deviations from Rouse behavior are therefore expected – the Rouse model deals with *linear* chains in bulk. Nevertheless, just to have an approximate idea of the range of characteristic frequencies involved in the problem, we may define a kind of 'equivalent' $W\ell^4$ parameter for the SCNPs in a first approximation equal to that in the equivalent Rouse chain. Analogous reasonings as for the precursor in the linear blend deliver for this parameter the dotted black curve in Fig. 8, with a Vogel-temperature value of 264 K. Also this 'equivalent' variable represents a much slower dynamics than the PEO-component in the nano-composite. As shown in the Supporting Information, the estimate of characteristic times associated to other correlation functions (self-motions of hydrogens, collective dynamics) of the components in the nano-composite point to similar differences. The slowing down of PEO Rouse modes in the mixtures might thus be attributed to the inferred dynamic asymmetry between the components, which persists at these high temperatures. The rigid PMMA-based component would impose a much higher effective friction to PEO chains in the mixture than similar flexible PEO chains do in the bulk material. Finally, we note that the revised Rouse description satisfactorily reproduces, within the experimental uncertainties, the Q-dependence of the PEO dynamic structure factor in the mixtures in the short-time regime. This means that the Q-dependence of the deviations with respect to bulk behavior is accounted for by a simple increase of the friction coefficient.

2. Local Reptation Regime

As can be clearly seen in Fig. 6, the impact of the presence of a polymer-based rigid component on PEO dynamics seems to be independent of the topology of that component for times below approx. 5 ns. However, PEO behavior becomes very different in the two mixtures at longer times. This is particularly emphasized if the NSE results are represented with the abscissa axis (time variable) in linear scale, as shown in Fig. 9. As previously commented, due to topological constraints imposed by the surrounding chains, at times longer than $\approx$ 10 ns

long PEO chains in bulk start deviating from Rouse behavior entering in the so-called local reptation regime. In Fig. 9, dashed lines represent the theoretical descriptions for bulk PEO results reported in Ref.[11] at the temperature here investigated (Eqs. 3-5 with $d_{tube}^{bulkPEO} =$ 5.3 nm and $W\ell^4 = 24150$ Å^4/ns). These curves also describe rather well the long-time ($t \geq 20$ ns approx.) behavior of PEO in the linear blend (empty symbols in the figure). This means that the extent of the localization of PEO chain motions is, within the experimental uncertainties, practically independent of being surrounded by other similar PEO chains or by a mixture of PEO chains and linear chains of the SCNPs-precursor.

The situation is very different for PEO in the nano-composite. In this case, $S_{chain}(Q,t)$ displays a much more pronounced decay (see filled symbols in Fig. 9), implying a significant increase of the explored volume of the polymer chain. Though constant plateaus are not actually reached within the explored NSE dynamic window, we may apply the reptation model in order to quantify the spatial extent of the chain motions. We have thus fitted the reptation expression (Eqs. 3-5) to the long-time NSE results fixing the value of the Rouse variable as that deduced from the short-time regime ($W\ell^4 = 17000$ Å^4/ns) and allowing the tube diameter to float. The obtained descriptions are shown in Fig. 10(a). A value of about 9.5 nm is deduced for the apparent tube diameter. We thus observe a huge increase (about 80%) of the spatial extent of the lateral chain motions with respect to the bulk system. We emphasize that this effective reduction of the constrains is a genuine consequence of the nano-particle nature of the PMMA-component: as it has been demonstrated in Fig. 9, in the linear blend this effect, if any, is very small. A fit of the reptation model to the linear blend NSE data, again fixing $W\ell^4 = 17000$ Å^4/ns) and allowing the tube diameter to float [Fig. 10(b)], reveals a tube diameter of about 6 nm, i. e., the increase of the tube diameter in the blend would amount to at most 13% of the bulk value.

Nowadays it is generally assumed that the effects of nano-particles on chain dynamics are of two kinds: (i) a 'direct' –also called 'geometrical'– effect due to nano-particle/chain interactions and (ii) an 'indirect' effect mediated by the induced orientational order in the polymer

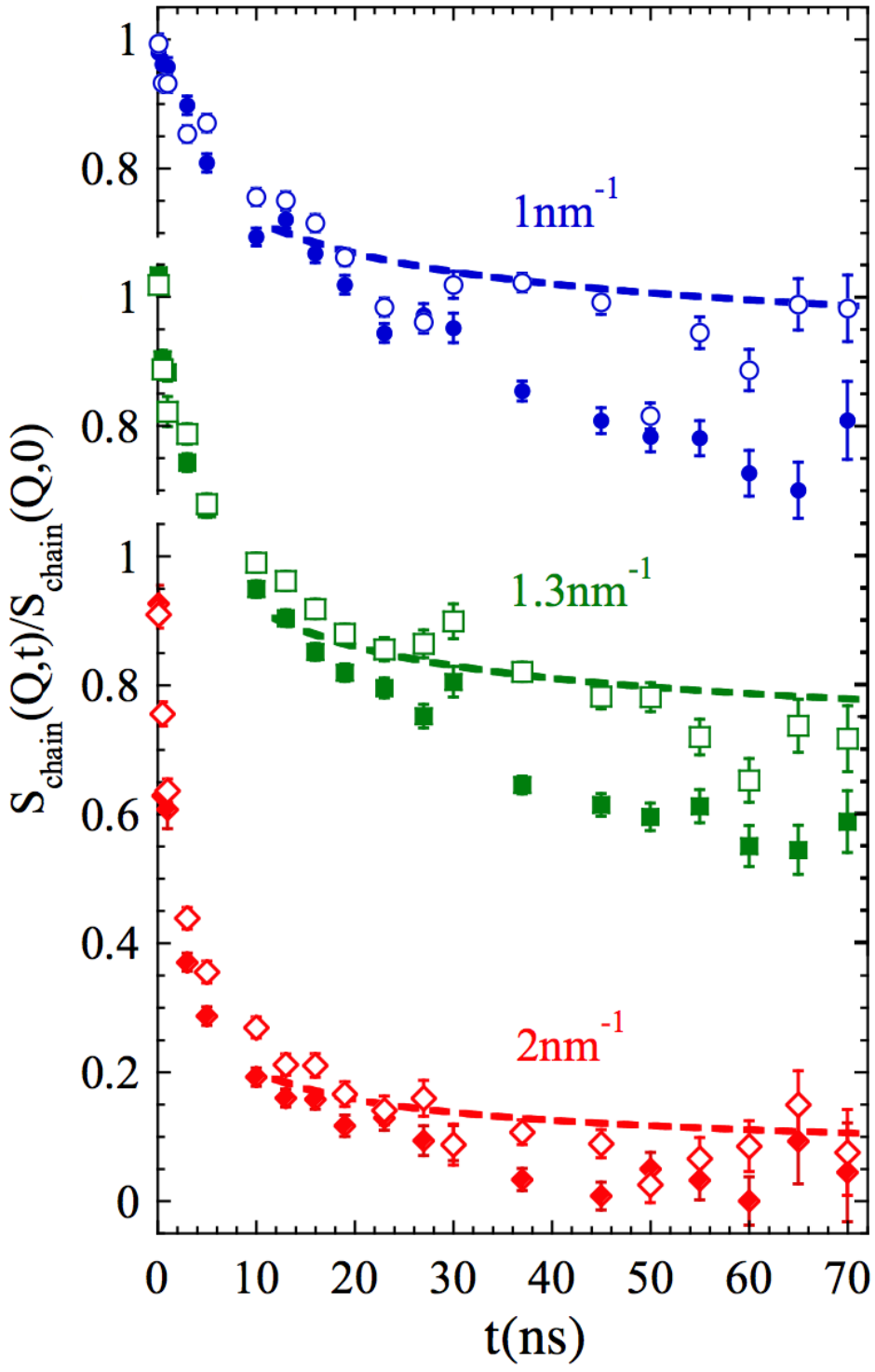

Figure 9: Normalized $S_{chain}(Q,t)$ of PEO chains in the nano-composite with SCNPs (filled symbols) and in the linear blend (empty symbols) at $Q = 1$ nm^{-1} (circles), 1.3 nm^{-1} (squares) and 2 nm^{-1} (diamonds). The abscissa (time) is represented in linear scale. Dashed lines display the reptation description of entangled PEO behavior in the bulk, which is found for times longer than 10 ns.[11]

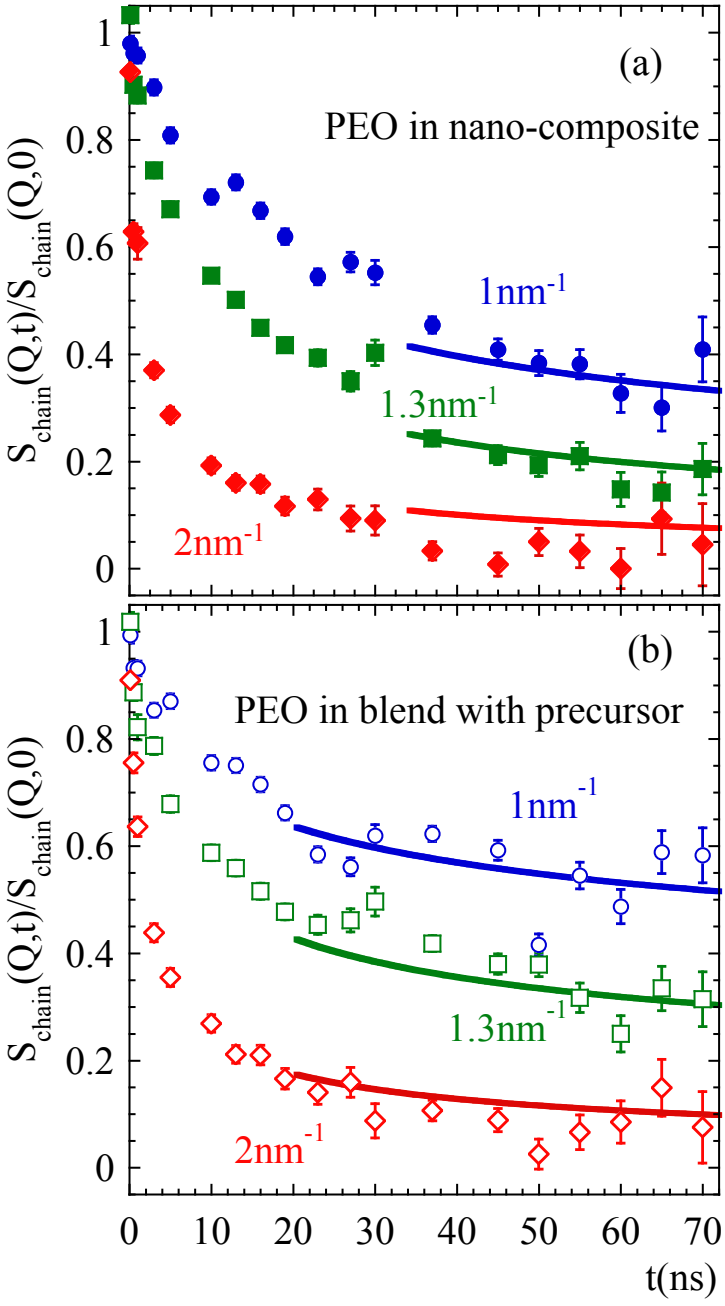

Figure 10: Normalized $S_{chain}(Q,t)$ of PEO chains in (a) the nano-composite and (b) the linear blend at the Q-values indicated. Solid lines are fits of the reptation model [Eqs. 3-5] to the experimental data for $t \geq 35$ ns in (a) and $t \geq 20$ ns in (b), fixing $W\ell^4 = 17000$ Å^4/ns and allowing the tube diameter d_{tube} to float. The resulting values are d_{tube}=9.5nm (a) and d_{tube}=6nm (b).

chain conformations. The way how both effects are superimposed is by no means trivial to treat, since it involves a complicated many-body problem.[48] A simple ansatz has been proposed to describe their combination, namely $d_{tube}^{-a} = d_{geo}^{-a} + d_{ent}^{-a}$. Here, the finally observed tube diameter (d_{tube}) is expressed as a function of that resulting from the presence of the obstacles (d_{geo}) and that imposed by the interactions with the rest of the chains (d_{ent}), which could be modified with respect to that in bulk through the 'indirect' effect. Obviously, in bulk polymers $d_{tube} = d_{ent}$. The exponent a is proposed to take values of 4[49] or 2. The latter approach seems to be supported by a theoretical study of rods/spheres-nano-composites[48] and was applied to NSE results on poly(ethylene propylene) (PEP) chains in a nano-composite with spherical silica nano-particles.[5] Starting from the measured apparent tube diameters $d_{tube}^{PEP/NC}$–which were always *smaller* than the bulk value $d_{tube}^{bulkPEP}$– and using an estimation for d_{geo} based on theoretical approaches,[50] the entanglement diameter $d_{ent}^{bulkPEP/NC}$ was obtained applying that ansatz. In this way, an increase of $d_{ent}^{bulkPEP/NC}$ with respect to $d_{tube}^{bulkPEP}$ was deduced for high nano-particle concentration. In our all-polymer nano-composite the geometrical impact is difficult to quantify, due to the peculiar topology of the SCNPs.[15,19–23] In a first rough approximation, we could represent our system as a nano-composite of spherical nano-particles with an effective nano-particle radius $R \approx \sqrt{(5/3)}\langle R_g \rangle \approx 7$ nm. The size of the nano-spheres ($2R \approx 14$ nm) would thus be rather similar to the unperturbed radius of gyration of the polymer chains ($\langle R_g^{bulkPEO} \rangle \approx 11.2$ nm). This situation was simulated by Li et al.,[7] who concluded that geometrical confinement is irrelevant for nano-particle concentration below $\phi_c \approx 32\%$. Hence, in our case the observed tube should be entirely determined by the constraints imposed by entanglements with other PEO chains, affected by the presence of the SCNPs ($d_{tube}^{PEO/NC} = d_{ent}^{PEO/NC}$). Note that if the geometrical confinement contribution could not be neglected ($1/d_{geo} \neq 0$), it would induce a reduction in the apparent tube diameter, implying that the entanglement tube should be even larger than that directly deduced from the experiments ($d_{ent}^{PEO/NC} > d_{tube}^{PEO/NC}$). Thus, the increase of the tube directly found in our case has to be necessarily attributed to a dilution of the entanglement

network, i. e., to indirect effects produced by the presence of the SCNPs. Comparing with the situation reported in Ref.,[5] to achieve a similar entanglement dilution effect as that here found for the all-polymer nano-composite, a volume fraction as high as about 50% of the spherical silica nano-particles used in that work should be considered. We note that for such system their experiments still reveal a smaller apparent tube than in bulk, attributed to the strong geometrical confinement component.

As suggested in Ref.,[5] two possible mechanisms might be invoked for entanglement tube dilation: (i) the high amount of particle surface provided by the nano-particles and (ii) confinement effects. Already about 20 years ago Silberberg[51,52] and Brown and Russell[53] proposed that the entanglement density is markedly reduced in the vicinity of a confining wall, as it is the case of interfaces. By contact with the interface, the local configurations of the polymer chain segments close to it are altered from the bulk configuration. The chain trajectory that would have occurred across the interface is reflected back into the polymer, and therefore the volume pervaded by a given chain length is smaller close to the wall than in the bulk. This reduces the entanglement density near the interface. As it has been mentioned in the Introduction, NSE experiments on long PEO polymer chains infiltrated in the cylindrical nano-pores of AAO membranes demonstrated the invoked tube dilation in the presence of confining walls.[6] Interestingly enough, the here observed effect is significantly larger than that reported under such well-defined confining geometry ($d_{tube}^{PEO/AAO}/d_{tube}^{bulkPEO} \approx 1.3$).

Given the expected rigidity of the SCNPs, their singularity compared to spherical nano-particles could be sought in their peculiar topology above commented. We might speculate that such morphology would be the origin of the observed behavior: on the one hand, the internal compaction of the SCNPs with respect to the precursors would exclude chain volume capable to form entanglements; on the other hand, protrusions of the SCNPs toward the surrounding macromolecules would offer a much larger amount of interface than the spherical nano-particles or the cylindrical regular walls of the AAO, contributing this enhancement of the interfacial regions also to the observed release of the topological constrains. In any case,

it is obvious that more efforts, from both experiments and simulations, are needed to fully understand the strong entanglement dilution effects reported here for the first time. This will be subject of future work.

IV. Conclusions

The structural analysis of the investigated mixture of long PEO linear chains and PMMA-based SCNPs has qualified it as a true nano-composite, i. e., a system where the two components are not mixed at a monomer level. The large-length scale insight into the macromolecular conformation of the SCNP in a PEO environment has shown a high compaction. Though a significant interpenetration of the components can be discarded, the small size of the nano-particles and their peculiar polydisperse topology favor the presence of a huge amount of interfaces in the mixture, inducing a clear plasticization effect on the SCNP.

The single chain dynamic structure factor of the PEO chains in this all-polymer nano-composite presents slowed down Rouse dynamics with respect to bulk PEO behavior for times below approx. 5 ns. The similar deceleration observed in the blend with linear precursor chains of the SCNPs points this effect to be a consequence of the large dynamic asymmetry in the mixtures as evidenced in the DSC traces. Thus, irrespective of their topology, the much slower PMMA-based macromolecules impose basically the same friction to PEO chain motions, much higher than that produced by similarly flexible PEO macromolecules.

The NSE results at longer times directly reveal a manifest increase of the explored volume of the polymer chain. The tube dilation effect has often been invoked for polymers under confinement. The spectacular disentanglement observed for PEO chain motions in this all-polymer nano-composite is much more pronounced than that reported for PEO in well-defined confining geometries and that deduced for PEP in nano-composites with spherical hard nano-particles, and absent in the blend with linear precursor chains. These observations lead to tentatively attribute the release of entanglements to the singular morphology of

SCNPs, through two mechanisms: (i) the decrease of chain volume susceptible of entangle the PEO chains due the internal compaction of the SCNPs and (ii) the increase of amount of interfaces leading to confinement effects.

Acknowledgements

We thank F. Lo Verso, A. J. Moreno, A. Alegría and K. S. Schweizer for fruitful discussions. Financial support from the Projects MAT2012-31088, MAT2015-63704-P and IT-654-13 (GV) is acknowledged. This work is based on experiments performed at JCNS-instrument JNSE (Heinz Maier-Leibnitz Zentrum (MLZ), Garching, Germany) and at SANS-1 (SINQ, Paul Scherrer Institute, Villigen, Switzerland), and has been supported by the European Commission under the 7th Framework Programme through the 'Research Infrastructures' action of the 'Capacities' Programme, NMI3-II Grant Number 283883.

References

(1) Rouse, P. E. A Theory of the Linear Viscoelastic Properties of Dilute Solutions of Coiling Polymers. *J. Chem. Phys.* **1953**, *21*, 1272

(2) Doi, M.; Edwards, S. F. *The Theory of Polymer Dynamics*; Clarendon Press:Oxford, 1986

(3) Richter, D.; Monkenbusch, M.; Arbe, A.; Colmenero, J. *Neutron Spin Echo in Polymer Systems*; Adv. Polym. Sci.; Springer Verlag, Berlin Heidelberg New York, 2005; Vol. 174

(4) de Gennes P. G. Reptation of a Polymer Chain in the Presence of Fixed Obstacles. *J. Phys. (Paris)* **1981**, *42*, 735

(5) Schneider, G.; Nusser, K.; Willner, L.; Falus, P.; Richter, D. Dynamics of Entangled Chains in Polymer Nanocomposites. *Macromolecules* **2011**, *44*, 5857

(6) Martín, J.; Krutyeva, M.; Monkenbusch, M.; Arbe, A.; Allgaier, J.; Radulescu, A.; Falus, P.; Maiz, J.; Mijangos, C.; Colmenero, J.; Richter, D. Direct Observation of Confined Single Chain Dynamics by Neutron Scattering. *Phys. Rev. Lett.* **2010**, *104*, 197801

(7) Li, Y.; Kröger, M.; Liu, W. K. Nanoparticle Effect on the Dynamics of Polymer Chains and Their Entanglement Network. *Phys. Rev. Lett.* **2012**, *109*, 118001

(8) Kim, D.; Srivastava, S.; Narayanan, S.; Archer, L. A. Polymer Nanocomposites: Polymer and Particle Dynamics . *Soft Matter* **2012**, *8*, 10813

(9) Mackay, M. E.; Dao, T. T.; Tuteja, A.; Ho, D. L.; van Horn, B.; Kim, H.-C.; Hawker, C. J. Nanoscale Effects Leading to Non-Einstein-like Decrease in Viscosity. *Nat. Mater.* **2003**, *2*, 762

(10) Tuteja, A.; Mackay, M. E.; Hawker, C. J.; Van Horn, B. Effect of Ideal, Organic Nanoparticles on the Flow Properties of Linear Polymers: Non-Einstein-like Behavior. *Macromolecules* **2005**, *38*, 8000

(11) Niedzwiedz, K.; Wischnewski, A.; Pyckhout-Hintzen, W.; Allgaier, J.; Richter, D.; Faraone, A. Chain Dynamics and Viscoelastic Properties of Poly(ethylene oxide). *Macromolecules* **2008**, *41*, 4866

(12) Hopkinson, I.; Kiff, F. T.; Richards, R. W.; King, S. M.; Farren, T. Isotopic Labelling and Composition Dependence of Interaction Parameters in Polyethylene Oxide/Polymethyl Methacrylate Blends. *Polymer* **1995**, *36*, 3523

(13) Colmenero, J.; Arbe, A. Segmental Dynamics in Miscible Polymer Blends: Recent Results and Open Questions. *Soft Matter* **2007**, *3*, 1474

(14) Bhowmik, D.; Pomposo, J. A.; Juranyi, F.; García-Sakai, V.; Zamponi, M.; Su, Y.; Arbe, A.; Colmenero, J. *Macromolecules* Microscopic Dynamics in Nanocomposites

of Poly(ethylene oxide) and Poly(methyl methacrylate) Soft Nanoparticles: A Quasi-Elastic Neutron Scattering Study. **2014**, *47*, 304

(15) Sanchez-Sanchez, A.; Akbari, S.; Etxeberria, A.; Arbe, A.; Gasser, U.; Moreno, A. J.; Colmenero, J.; Pomposo, J. A. Michael Nanocarriers Mimicking Transient-Binding Disordered Proteins. *ACS Macro Lett.* **2013**, *2*, 491

(16) Fetters, L. J.; Lohse, D. J.; Milner, S. T.; Graessley, W. W. Packing Length Influence in Linear Polymer Melts on the Entanglement, Critical, and Reptation Molecular Weights. *Macromolecules* **1999**, *32*, 6847

(17) Mezei, F. *Lecture Notes in Physics*; Springer-Verlag Berlin, Heidelberg, New York, 1980

(18) Bhowmik, D.; Pomposo, J. A.; Juranyi, F.; Garcia-Sakai, V.; Zamponi, M.; Arbe, A.; Colmenero, J. nvestigation of a Nanocomposite of 75 wt % Poly(methyl methacrylate) Nanoparticles with 25 wt % Poly(ethylene oxide) Linear Chains: A Quasielatic Neutron Scattering, Calorimetric, and WAXS Study. *Macromolecules* **2014**, *47*, 3005

(19) Sanchez-Sanchez, A.; Akbari, S.; Moreno, A. J.; Lo Verso, F.; Arbe, A.; Colmenero, J.; Pomposo, J. A. Design and Preparation of Single-Chain Nanocarriers Mimicking Disordered Proteins for Combined Delivery of Dermal Bioactive Cargos. *Macromol. Rapid Commun.* **2013**, *34*, 1681

(20) Perez-Baena, I.; Barroso-Bujans, F.; Gasser, U.; Arbe, A.; Moreno, A. J.; Colmenero, J.; Pomposo, J. A. Endowing Single-Chain Polymer Nanoparticles with Enzyme-Mimetic Activity. *ACS Macro Lett.* **2013**, *2*, 775

(21) Moreno, A. J.; Lo Verso, F.; Sanchez-Sanchez, A.; Arbe, A.; Colmenero, J.; Pomposo, J. A. Advantages of Orthogonal Folding of Single Polymer Chains to Soft Nanoparticles. *Macromolecules* **2013**, *46*, 9748

(22) Lo Verso, F.; Pomposo, J. A.; Colmenero, J.; Moreno, A. J. Multi-Orthogonal Folding of Single Polymer Chains into Soft Nanoparticles. *Soft Matter* **2014**, *10*, 4813

(23) Pomposo, J. A.; Perez-Baena, I.; Lo Verso, F.; Moreno, A. J.; Arbe, A.; Colmenero, J. How Far Are Single-Chain Polymer Nanoparticles in Solution from the Globular State?. *ACS Macro Letters* **2014**, *3*, 767

(24) Hammouda, B. Small-Angle Scattering From Branched Polymers. *Macromolecular Theory and Simulations* **2012**, *21*, 372

(25) Moreno, A. J.; LoVerso, F.; Arbe, A.; Pomposo, J. A.; Colmenero, J. Concentrated Solutions of Single-Chain Nanoparticles: A Simple Model for Intrinsically Disordered Proteins under Crowding Conditions. *J. Phys. Chem. Lett.* **2016**, *7*, 838

(26) Grosberg, A. Y.; Nechaev, S. K.; Shakhnovitch, E. I. The Role of Topological Constraints in the Kinetics of Collapse of Macromolecules. *J. Phys. (Paris)* **1988**, *49*, 2095

(27) Fetters, L. J.; Lohse, D. J.; Richter, D.; Witten, T. A.; Zirkel, A. Connection between Polymer Molecular Weight, Density, Chain Dimensions, and Melt Viscoelastic Properties. *Macromolecules* **1994**, *27*, 4639

(28) Leroy, E.; Alegría, A.; Colmenero, J. Quantitative Study of Chain Connectivity Inducing Effective Glass Transition Temperatures in Miscible Polymer Blends. *Macromolecules* **2002**, *35*, 5587

(29) Sakaguchi, T.; Taniguchi, N.; Urakawa, O.; Adachi, K. Calorimetric Study of Dynamical Heterogeneity in Blends of Polyisoprene and Poly(vinylethylene). *Macromolecules* **2005**, *38*, 422

(30) Miwa, Y.; Usami, K.; Yamamoto, K.; Sakaguchi, M.; Sakai, M.; Shimada, S. Direct Detection of Effective Glass Transitions in Miscible Polymer Blends by Temperature-Modulated Differential Scanning Calorimetry. *Macromolecules* **2005**, *38*, 2355

(31) Herrera, D.; Zamora, J. C.; Bello, A.; Grimau, M.; Laredo, E.; Müller, A. J.; Lodge, T. Miscibility and Crystallization in Polycarbonate/Poly(ϵ-caprolactone) Blends: Application of the Self-Concentration Model. *Macromolecules* **2005**, *38*, 5109

(32) Lodge, T. P.; Wood, E. R.; Haley, J. C. Two Calorimetric Glass Transitions Do Not Necessarily Indicate Immiscibility: The Case of PEO/PMMA. *J. Polym. Sci.: Part B: Polym. Phys.* **2006**, *44*, 756

(33) Chung, G.-C.; Kornfield, J. A.; Smith, S. D. Component Dynamics Miscible Polymer Blends: A Two-Dimensional Deuteron NMR Investigation. *Macromolecules* **1994**, *27*, 964

(34) Chung, G.-C.; Kornfield, J. A.; Smith, S. D. Compositional Dependence of Segmental Dynamics in a Miscible Polymer Blend. *Macromolecules* **1994**, *27*, 5729

(35) Lodge, T. P.; McLeish, T. C. B. Self-Concentrations and Effective Glass Transition Temperatures in Polymer Blends. *Macromolecules* **2000**, *33*, 5278

(36) Zetsche, A.; Fischer, E. W. Dielectric Studies of the α-Relaxation in Miscible Polymer Blends and its Relation to Concentration Fluctuations. *Acta Polym.* **1994**, *45*, 168

(37) Katana, G.; Fischer, E. W.; Hack, T.; Abetz, V.; Kremer, F. Influence of Concentration Fluctuations on the Dielectric α-Relaxation in Homogeneous Polymer Mixtures. *Macromolecules* **1995**, *28*, 2714

(38) Kumar, S. K.; Colby, R. H.; Anastasiadis, S. H.; Fytas, G. Concentration Fluctuation Induced Dynamic Heterogeneities in Polymer Blends. *J. Chem. Phys.* **1996**, *105*, 3777

(39) Kamath, S.; Colby, R. H.; Kumar, S. K.; Karatasos, K.; Floudas, G.; Fytas, G.; Roovers, J. E. L. Segmental Dynamics of Miscible Polymer Blends: Comparison of the Predictions of a Concentration Fluctuation Model to Experiment. *J. Chem. Phys.* **1999**, *111*, 6121

(40) Salaniwal, S.; Kant, R.; Colby, R. H.; Kumar, S. K. Computer Simulations of Local Concentration Variations in Miscible Polymer Blends. *Macromolecules* **2002**, *35*, 9211

(41) Kamath, S.; Colby, R. H.; Kumar, S. K. Evidence for Dynamic Heterogeneities in Computer Similations of Miscible Polymer Blends. *Phys. Rev. E* **2003**, *67*, 010801(R)

(42) Kamath, S.; Colby, R. H.; Kumar, S. K. Dynamic Heterogeneity in Miscible Polymer Blends with Stiffness Disparity: Computer Simulations Using the Bond Fluctuation Model. *Macromolecules* **2003**, *36*, 8567

(43) Kant, R.; Kumar, S. K.; Colby, R. H. What Length Scales Control the Dynamics of Miscible Polymer Blends?. *Macromolecules* **2003**, *36*, 10087

(44) Brodeck, M.; Alvarez, F.; Arbe, A.; Juranyi, F.; Unruh, T.; Holderer, O.; Colmenero, J.; Richter, D. Study of the Dynamics of Poly(ethylene oxide) by Combining Molecular Dynamic Simulations and Neutron Scattering Experiments. *J. Chem. Phys.* **2009**, *130*, 094908

(45) Allegra, G.; Ganazzoli, F. Chain Conformation and Dynamics in the Gaussian Approximation. *Adv. Chem. Phys.* **1989**, *75*, 265

(46) Genix, A.-C.; Arbe, A.; Alvarez, F.; Colmenero, J.; Willner, L.; Richter, D. Dynamics of Poly(ethylene oxide) in a Blend with Poly(methyl methacrylate): A Quasielastic Neutron Scattering and Molecular Dynamics Simulations Study. *Phys. Rev. E* **2005**, *72*, 031808

(47) Bergman, R.; Alvarez, F.; Alegría, A.; Colmenero, J. Dielectric Relaxation in PMMA Revisited. *J. Non-Cryst. Solids* **1998**, *235-237*, 580

(48) Yamamoto, U.; Schweizer, K. S. Theory of Entanglements and Tube Confinement in Rod-Sphere Nanocomposites. *ACS Macro Letters* **2013**, *2*, 955

(49) Mergell, B.; Everaers, R. Tube Models for Rubber-Elastic Systems. *Macromolecules* **2001**, *34*, 5675

(50) Torquato, S.; Lu, B.; Rubinstein, J. Nearest-Neighbor Distribution Functions in Many-body Systems. *Phys. Rev. A* **1990**, *41*, 2059

(51) Silberberg, A. Distribution of Conformations and Chain Ends near the Surface of a Melt of Linear Flexible Macromolecules. *J. Colloid Interface Sci.* **1982**, *90*, 86

(52) Silberberg, A. Distribution of Segments near the Surface of a Melt of Linear Flexible Macromolecules: Effect on Surface Tension. *J. Colloid Interface Sci.* **1988**, *125*, 14

(53) Brown, H. R.; Russell, T. P.. Entanglements at Polymer Surfaces and Interfaces. *Macromolecules* **1996**, *29*, 798

FOR TABLE OF CONTENTS USE ONLY

'Single Chain Dynamic Structure Factor of Linear Polymers in an All-Polymer Nano-Composite'

Arantxa Arbe, José A. Pomposo, Isabel Asenjo-Sanz, Debsindhu Bhowmik, Oxana Ivanova, Joachim Kohlbrecher and Juan Colmenero